[CH]

Convection and crystallization in magma cooled from above

M. Grae Worster [a,1], Herbert E. Huppert [a,b] and R. Stephen J. Sparks [c]

[a] *Department of Applied Mathematics and Theoretical Physics, University of Cambridge, Silver Street, Cambridge CB3 9EW, U.K.*
[b] *Institute of Theoretical Geophysics, University of Cambridge, 20 Silver Street, Cambridge CB3 9EW, U.K.*
[c] *Department of Geology, Wills Building, University of Bristol, BS8 1RJ, U.K.*

ABSTRACT

Calculations are presented for the cooling from above of melts in the Di–An system in which the kinetics of crystallization are incorporated and play a dominant role. The results indicate that even with no initial superheat whatsoever, convection plays an important role in the cooling of magma chambers and allows substantial internal cooling, crystallization and differentiation. The calculations show, in agreement with observations, that in magma bodies hundreds of meters thick, crystallization occurs predominantly in the interior or at the floor, even though heat is lost only from the roof. The ratio of the final thickness of the layer formed at the floor to that formed at the roof increases as the overall size of the chamber increases, owing to the effects of convection.

1. Introduction

Ever since the pioneering papers by Shaw [1] and Bartlett [2] it has been widely appreciated that convection is an important dynamical process in magma chambers. When homogeneous magma is cooled from above, the very large dimensions of typical chambers ensures that the Rayleigh number based on the depth of the chamber H is much larger than that required for vigorous convection to occur. A large number of papers depending upon this fact have appeared in the refereed literature since then (see, for example Carrigan [3] Brandeis and Jaupart [4], McBirney [5] and references therein). However, this picture has recently been challenged by Brandeis and Marsh [6] and Marsh [7] who suggest in contrast that convection is weak or nonexistent in almost all magma chambers, which implies also that differentiation cannot occur in magma chambers. The two principal arguments they put forward are first, that magma chambers are cooled predominantly from above

by conduction through solid roof rocks and secondly, that crystallization at the roof largely prevents the destabilization of the resulting cooled magma from driving convection. The current paper demonstrates that the second conclusion is unwarranted.

Our work examines the application of a theoretical model for the cooling and crystallization of a binary system from above in which the all-important kinetics of crystal growth are taken into account. The results, as discussed in section 4, demonstrate that vigorous convection, significant internal cooling and differentiation can take place in a magma chamber which is cooled by losing heat by conduction to the overlying country rocks even when there is no initial superheat. In addition, as we outline in section 5, the interpretations of our theoretical calculations are consistent with many geological observations of intrusions. In particular, the incorporation of kinetic effects allows us to explain how solidification can take place at the floor of the chamber even though the cooling takes place at the roof. In fact, the desire to understand this field observation acted as the major motivation for the investigations reported in this paper.

---

[1] Present address: Department of Engineering Science and Applied Mathematics, and Department of Chemical Engineering, Northwestern University, Evanston, IL 60208, U.S.A.

2. Background

A study of the solidification of magma cooled from above, that includes the effects of convection, was presented by Turner et al. [8]. Their theoretical model assumed equilibrium crystallization and so, with the absence of any kinetic undercooling, convection was driven solely by the temperature difference between the liquidus and the superheated magma. They showed analytically, and confirmed experimentally, that the thermal balance between conduction, convection and the removal of superheat changes with time and, in particular, that the rapid heat transfer associated with turbulent convection causes the superheat to be reduced to small values after a relatively short time. Thereafter the dominant thermal balance controlling the rate of solidification near the roof is between conduction and the removal of latent heat, even though there still remains vigorous convection in the fluid interior of the chamber.

This paper presents extensions and applications of a theoretical and experimental model developed by Kerr et al. [9–12] for the crystallization of a binary eutectic system cooled from above in which the kinetics of crystal growth are taken into account, the importance of which was already realised by Brandeis and Jaupart [4]. In order for crystals to grow, the temperature at the interface between the crystals and the melt must be less than the liquidus temperature of that melt. Usually the departures from thermodynamic equilibrium are small in comparison with the typical variations of temperature within the system and, in the absence of convection, are confined to the near neighbourhood of the interface. They can therefore often be ignored, and good theoretical results can be obtained by employing equilibrium thermodynamics. However, convection can play an important role in transporting (relatively dense) undercooled fluid from the neighbourhood of the solidification front into the interior of the chamber, and this has significant consequences for the evolution of the magma within the chamber. We apply the model to cases in which there is initially no superheat whatsoever, so that the kinetic undercooling is the sole cause of convection as well as the principal quantity of interest being transported by the flow.

During the solidification of a binary system, partially solidified regions generally form. We assume here that these take the form of mushy zones of connected crystals. This contrasts with the investigations by Huppert and Sparks [13–15] in which the authors implicitly assumed that crystals grew in suspension in the form of a slurry and were immediately swept away by the convection. These two pictures represent extreme cases of possible behaviour and must be analysed separately. The cases in which attached mushy layers form differ in two important ways from cases in which crystals grow in suspension. First, if there is no transfer of crystals from a mushy zone to the interior then any crystallization in the interior can only result from undercooling and nucleation in that region. Secondly, the temperature differences available to drive convection are much smaller when a mushy layer forms. Nevertheless, we shall see that the temperature differences are sufficiently large to produce vigorous convection. A third distinction between the present paper and those of Huppert and Sparks [13–15] is that our assumption of no superheat prevents any possibility of remelting the mushy zone.

3. Analysis

A brief summary below describes the essential physics and the principal results of the theoretical analysis and supporting experimental observations of Kerr et al. [9–12]. The results are then specifically applied to the growth of diopside crystals from a Di–An melt, because there is extensive information on thermochemical properties [16] and kinetic growth rates [17] for this system. While the Di–An system is a simplification of naturally occurring rock, it is the only system known to us for which values of the appropriate physical parameters have been evaluated.

A melt at its liquidus temperature placed against a cold, solid roof will begin to crystallize as heat is conducted into the overlying rock. If the temperature T_b at the position of the initial contact between melt and country rock ($z = 0$) is less than the eutectic temperature of the melt T_e then a crust of composite solid will grow (Fig. 1). Below the level $z = h_e$ at which $T = T_e$, a mushy layer forms comprising crystals and depleted interstitial liquid. Here we consider only the case when the crystals remain attached to the roof to form a
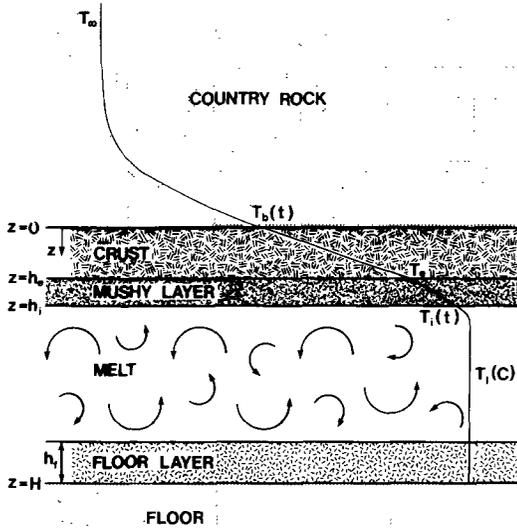
Fig. 1. Schematic diagram of an intrusion being cooled from above. Heat is conducted into the country rock above the roof at $z = 0$. As the magma is cooled it crystallizes to form a crust of composite solid above a mushy layer. The molten magma convects vigorously as it cools with internal crystallization producing a solid layer near the floor. A sketch of the temperature field is indicated on the diagram.

connected matrix and the interstitial liquid is buoyant so that it remains trapped within the mushy layer. The crystals at the interface between the mushy layer and the melt ($z = h_i$) grow only when the temperature there, T_i, is below the liquidus temperature of the melt T_L.

Crystal growth rates depend on local thermodynamic factors related to attachment mechanisms and vary from system to system. For diopside growing into its undercooled melt, the growth law for the rate of increase of crystalline solid, $\dot{h}_i$, is given by

$$\dot{h}_i = G\mu^{-1}(\Delta T)^2, \tag{1}$$

where $\Delta T = T_L - T_i$ is the interfacial undercooling and $G = 5.6 \times 10^{-5}$ cm s^{-1} °C^{-2} poise [18, after correcting a typographical error imaginatively spotted and reported to us by Becky Renner]. This growth law is expressed in terms of the dynamic viscosity μ of the molten diopside, which we approximate by the function

$$\mu = \exp[(12 - 52.5x + 62.5x^2)\ln 10], \tag{2}$$

where $x = 1 - 1000/T$ and T is the absolute temperature of the melt measured in Kelvin. We de-

rived this expression by fitting a curve to the graphical data of Kirkpatrick [18]. We use expression (2) in relation (1) for all our calculations of diopside growing from a Di–An melt. In section 5 we shall discuss how the growth law might vary as a function of composition and what effect such variations would have on our conclusions. In the absence of any superheat, it is the interfacial undercooling that drives thermal convection in the melt. The convection cools the entire region of melt to cause internal growth of crystals in addition to those which form near the roof. These may form and remain in suspension, may settle on the floor or may simply form and grow at the floor and other margins. We assume that the additional crystallization below the roof occurs at the bottom of the chamber to form a solid layer of depth $h_f(t)$. The residual liquid released by the growing floor layer is buoyant and rises convectively to mix with the interior of the melt. Thus the composition of the melt evolves with time in such a way as to lower its liquidus temperature and counteract the undercooling caused by the thermal convection driven from above.

In order to understand the dynamical behaviour of the system described in Fig. 1 and the preceding paragraphs, it is important to appreciate the location and magnitude of the temperature and compositional variations that exist. There is a temperature variation of many hundreds of degrees centigrade across the composite solid layer, which, from a dynamical point of view, is totally inactive. A further variation, of up to a few hundred degrees, which reflects the difference between the eutectic and liquidus temperatures, exists across the mushy layer. This partially solidified region has been considered by some authors to be part of the thermal boundary layer at the cooled roof of magma chambers and there have been a number of discussions about how much of this region participates in convection (see, for example, Carrigan [3], Stengel et al. [19] and Richter et al. [20]). Alternatively, one can assume, as does Bruce [21], that this region is a mobile slurry of unconnected crystals. He concluded that much of this region is nevertheless stagnant, because there is a strong variation of the viscosity of the magma with temperature. Here we take the view that none of this region participates in convection, either for the reasons stated above or

because the mushy layer comprises a matrix of connected crystals. This is the same interpretation as that made by Brandeis and Marsh [6] and Marsh [7]. Finally, there may be a temperature variation ΔT across the narrow thermal boundary layer ahead of the advancing interface between the mushy layer and the completely liquid region. It is this temperature variation which drives any thermal convection in the liquid region. The existence and strength of convection is determined by the magnitude of a Rayleigh number Ra based on this ΔT and the total depth of the liquid region, as discussed further below.

If the assumptions of equilibrium thermodynamics are made, then the temperature at the interface of the mushy layer with the melt, T_i, is equal to the liquidus temperature of the melt. Only two possibilities then exist: either the melt is superheated, in which case it has been shown analytically [8–12] and experimentally [5,8–12] that the melt cools rapidly by convection to temperatures close to the liquidus temperature; or the magma is not superheated, in which case there is no convection. In the former case, references [8] and [10] show that vigorous convection continues for most of the evolution of the chamber, even though the temperature difference driving the convection is very small and the convective heat transfer from the melt is small in comparison with the conductive heat transfer through the mushy layer.

In the present paper the superheat of the magma is assumed to be identically zero. Convection is driven only by the kinetic undercooling associated with the solidification of crystals at the edge of the mushy layer, which causes T_i to be always less than the liquidus temperature of the melt and hence ΔT to be always non-zero. A feature of the mushy layer is that it incorporates all of the compositionally depleted liquid generated by the solidification. This is appropriate in the geologically relevant parameter range in which the compositional diffusivity is very much less than the thermal diffusivity. The negative buoyancy due to the thermal variation ΔT is thus not counteracted by any compositional buoyancy within the thermal boundary layer. We shall also see later that the kinetic undercooling ΔT is only a few degrees centigrade at most, so it is appropriate to assume that the viscosity of the melt is spatially (but not

temporally) thermally) uniform throughout the liquid region, including the thermal boundary layer. The Rayleigh number governing convection in the melt should therefore be based upon the thermal buoyancy alone, the depth of the liquid region $H_1 = H - h_i - h_f$, and the kinematic viscosity of the melt ν. It thus scales as

$$Ra = \frac{\alpha g \Delta T H_1^3}{\kappa \nu}$$

where α is the coefficient of thermal expansion, g is the acceleration due to gravity and κ is the thermal diffusivity of the melt. The driving temperature difference ΔT, due to kinetic undercooling, is related to the rate of solidification of the mushy layer through (1). The result of computing this expression for the Rayleigh number is presented as a function of time in section 4. We simply note here that, for typical magmatic parameter values, its magnitude is very much greater than that required for vigorous convection within the melt.

The evolution of this system is thermally controlled and in order to conduct a quantitative analysis we need appropriate equations for each region. Conduction governs heat transfer in the country rock and the composite layer. Since the country rock warms up from its initial, uniform temperature T_∞ by heat transferred from the hot magma, the temperature T_b at the boundary with the country rock varies with time as described in the appendix of [13]. In the mushy layer, conduction balances the internal release of latent heat caused by local increases in the solid fraction ϕ, which is determined in part by the local conservation of solute. Equations for this region were derived by Worster [22]. At the interface between the mushy layer and the melt, the conductive flux into the mushy layer is given by

$$k\frac{\partial T}{\partial z} = \phi L \dot{h}_i + c_1 \Delta T \dot{h}_i + F \tag{3}$$

where k is a thermal conductivity for the mushy layer. The first term on the right hand side of (3) represents the latent heat released at the interface, where L is the latent heat per unit volume of solid grown. The second term represents the specific heat in the thermal boundary layer ahead of the growing mushy layer, where c_1 is the specific heat per unit volume of liquid. The third term repre-

TABLE 1

Values of physical properties used in the calculations

			Melt	Solid diopside	Solid anorthite	Country rock
Density	ρ	g cm^{-3}	2.60	2.69	2.65	2.60
Specific heat capacity	C_p	cal g^{-1} °C^{-1}	0.380	0.273	0.274	0.380
Latent heat	L	cal g^{-1}	–	159	94	–
Conductivity	k	cal cm^{-1} s^{-1} °C^{-1}	8×10^{-3}	8×10^{-3}	8×10^{-3}	8×10^{-3}
Kinematic viscosity	ν	cm^2 s^{-1}	10	–	–	–
Coeff. of thermal expansion	α	°C^{-1}	1.1×10^{-4}	–	–	–

sents the convective heat transfer from the melt and is given [23] by

$$F = 2^{4/3}\lambda k(\alpha g/\kappa \nu)^{1/3}\Delta T^{4/3} \qquad (4)$$

where λ is an empirical constant, taken to be 0.056, α is the coefficient of thermal expansion, g is the acceleration due to gravity, κ is the thermal diffusivity and ν is the kinematic viscosity of the melt. We compute the kinematic viscosity from the expression

$$\nu = \frac{1}{\rho_1}\exp\left[\left(1.5 + \frac{1345 - T}{122}\right)\ln 10\right] \qquad (5)$$

where T, here, is measured in °C and ρ_1 is the density of the melt. This expression is derived by fitting the graphical data for viscosities along the liquidus curve given by Weill et al. [16].

The convective heat flux also serves to cool the interior of the magma and to grow crystals there, a process expressed by the equation

$$F = -C\dot{T}_1 + L\dot{h}_f \qquad (6)$$

where T_1 is the uniform temperature of the melt and C is the total heat capacity of the region below $z = h_i$. The second term on the right-hand side of (6) represents the latent heat required to produce internal crystallization, the rate of which is determined implicitly by assuming that it is sufficiently rapid to keep the melt at its liquidus temperature. Thus

$$T_1 = T_L(C) \qquad (7)$$

where C is the composition of the melt, which is related to the depth of the floor layer by global conservation of solute. This is expressed as

$$(C_f - C)\dot{h}_f = (H - h_i - h_f)\dot{C} \qquad (8)$$

where C_f is the composition of the solid forming

the crystals at the floor (in this case pure diopside) and H is the total depth of the system.

Further details of the analytical model can be found in [10–12] and an extended summary appears in [9]. The consequences of the model have also been carefully tested and are supported by the very good agreement between the theoretical predictions and the results of experiments on the cooling of aqueous solutions. Although the kinetic growth laws for aqueous solutions can be different in form from those in the Di–An system or a more complex magma, the essential physical principles are identical. The physical parameters we have used in our calculations come from [16] and are listed in Table 1. Properties of multi-phase regions are calculated using local averages weighted by the volume fractions of the constituent phases.

4. Results

One of the principal roles of convection is illustrated by Fig. 2, which shows the depths of solid grown at the roof and the floor as functions of time from a melt of pure diopside in a layer initially 100 m thick. A comparison is made between the predictions of the model with and without convection. The non-convective case is neither physically nor geologically relevant, since the Rayleigh number is very large ($\sim 10^{14}$), but it serves as a basis for comparison. Convection reduces the time for complete solidification by about 30%. We note that the difference between the two predictions for the growth of solid at the roof is small, certainly in comparison with the uncertainties in current field measurements. This demonstrates the fact that the dominant thermal balance governing growth of the roof solid is that between

conduction and the release of latent heat [8]. Despite this observation, vigorous convection of the melt persists and, most significantly, the convective mixing of undercooled liquid from near the roof into the interior of the chamber causes some 45% of the chamber to solidify at the floor, even though it is being cooled only from the roof.

Note that because the time scale for solidification is not significantly altered by the presence of convection in the melt, any argument for the existence (or absence) of convection that is based only on an agreement between observations and theoretical predictions of solidification rates cannot be soundly based. The effects of convection in the melt may only be clearly seen in the final, differentiated product, as determined below.

Figure 3 shows results for the solidification of a magma of composition $Di_{80}An_{20}$ for three different depths of chamber. There are several interesting features. After a very early transient period, not visible in the figures, a mushy layer develops below a composite solid layer near the roof and a pure solid layer develops at the floor. Each of these evolves until the temperature of the liquid region reaches the eutectic, after which time the growing roof is completely solid, i.e. there is no longer a mushy layer. Further removal of heat from the interior by convective heat transfer to the roof results in the internal crystallization of

Fig. 3. The growth of solid as a function of time for a magma of composition $Di_{80}An_{20}$ intruded into country rock initially at $0\,^\circ$C. The different phases are shown with different shadings and labelled in (a). A composite solid of vertically oriented diopside and anorthite crystals forms near the roof above a mushy layer of diopside crystals and interstitial melt. A layer of pure diopside forms near the base of the intrusion at early times and is overlain by a composite layer of randomly oriented crystals later on. The three diagrams indicate the different evolutions experienced by intrusions of different initial depths H. (a) $H = 10$ m; (b) $H = 100$ m; (c) $H = 1000$ m.
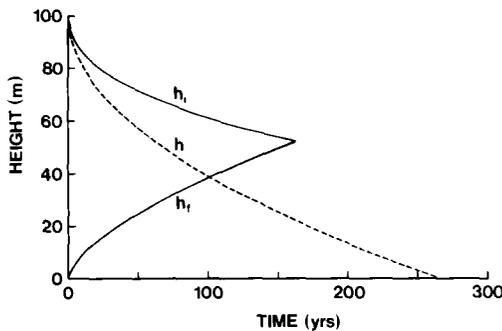

Fig. 2. The growth of solid as a function of time for pure diopside at its melting temperature intruded as a layer 100 m thick into country rock at $0\,^\circ$C. The dashed curve shows the prediction of a purely conductive calculation for the depth of the solid roof layer, h. The solid curves show the predictions of a more realistic calculation in which vigorous convective heat transfer is taken into account. Solid grows in the interior of the intrusion to form a layer of height h_f at the base in addition to a layer of thickness h_i attached to the roof. The basal layer forms even though the cooling is through the roof only.
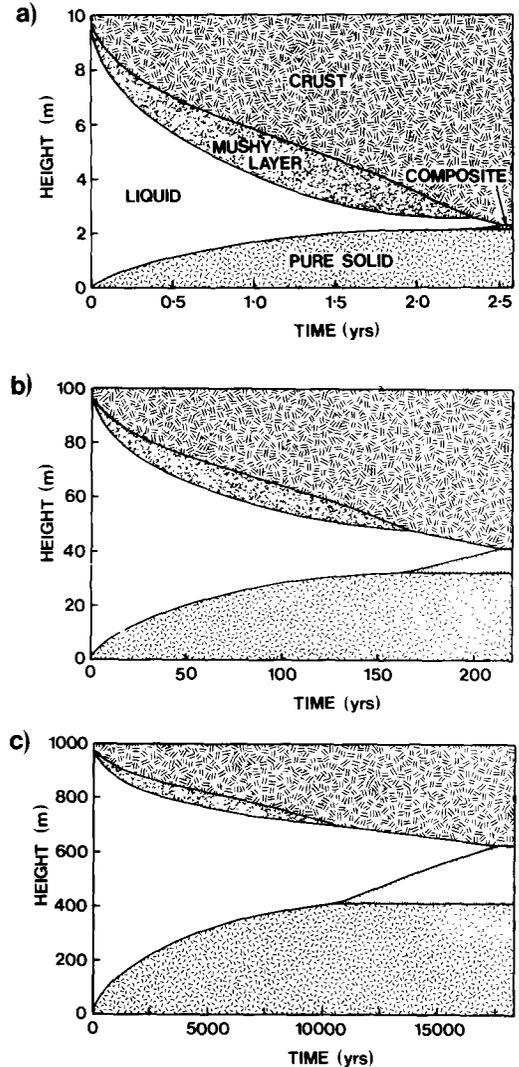
anorthite in addition to the diopside crystals already forming. Thus, a composite layer whose composition is equal to the eutectic ($Di_{58}An_{42}$) forms at the floor, with the appropriate release of latent heat, while the interior temperature remains
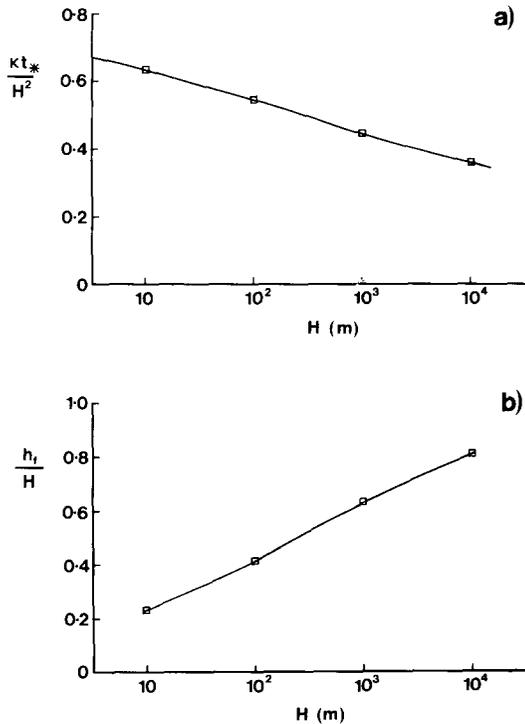
Fig. 4. Results for a magma of composition $Di_{80}An_{20}$ intruded at its liquidus into country rock initially at $0°C$. (a) The ratio $\kappa t_*/H^2$ as a function of the initial depth of the intrusion H, where t_* is the time taken for complete solidification. This ratio would be constant (~ 0.69) if the heat transfer were purely conductive. The ratio decreases as H increases and convective heat transfer becomes more important. (b) The ratio of the final depth of the layer formed near the floor h_f to the total depth of the intrusion H as a function of H.

fixed at the eutectice value ($1274°C$). The increased crystallization that occurs once the interior magma has achieved the eutectic temperature and concentration is reflected in the marked increase in the rate of growth of solid at the floor.

Significant variations in the evolution of the chamber depending on its total depth can be seen by comparing the results in Fig. 3. Two important variations are illustrated further in Fig. 4. Figure 4a shows the dimensionless time $\kappa t_*/H^2$, for complete solidification as a function of the initial depth of the chamber, H, where t_* is the actual time taken for complete solidification. Since t_* has been scaled with the conductive time scale H^2/κ, this ratio would be constant (~ 0.69) if conduction were the sole means of heat transfer. The decrease of $\kappa t_*/H^2$ with increasing H, while not large, is easily sufficient to demonstrate clearly the

increasing role of convection as the depth of the chamber increases. Convection has two effects on the solidification. By increasing the heat transfer from the melt to the roof, it inhibits growth of the mushy layer and roof solid. By increasing the cooling of the melt, it enhances the internal growth of crystals (here at the floor). Thus as the height of the chamber increases and the intensity of the convective flow correspondingly increases, more of the solidification occurs at the floor rather than at the roof. This is illustrated in Fig. 4b, where the fraction of the depth of the chamber occupied by solid grown at the floor is plotted against the depth of the chamber. Note that if the internal crystal growth were to occur in suspension and the crystals settled to the floor to form a loosely packed layer then this fraction would increase. The fraction would further increase if cooling also took place through the floor.

The structure of the solidified magma chamber can vary considerably depending upon the initial composition of the magma. In Fig. 5 we compare the evolution of three identical chambers of height 100 m which contain magmas of different initial compositions (and thus also temperatures). The time for complete freezing increases, though only slightly, as the magma is more enriched in diopside. More significantly, we see that when the initial composition is close to the eutectic concentration (Fig. 5a) most of the chamber has a composite mineralogy, having formed either as crust from the roof or as a eutectic composite from the floor. By contrast, when the magma has initial composition $Di_{95}An_5$ (Fig. 5c) there is no eutectic composite grown at the floor.

The evolution of the temperature of the melt for a 100 m thick layer of $Di_{80}An_{20}$ is shown in Fig. 6a. Since, by assumption, there is no superheat, the temperature can only decrease in conjunction with the changing composition, and hence liquidus temperature, of the melt caused by the internal crystallization. No further decrease in the temperature of the melt is possible below the eutectic temperature, which is reached after about 130 years in the example illustrated. Also shown in Fig. 6a is the temperature of the interface between the mushy layer and the melt, which is always less than the temperature of the melt itself. The difference between these temperatures ΔT is shown in Fig. 6b. Despite the fact that ΔT is so

small, it leads to large values of the Rayleigh number and is sufficient for there to be vigorous convection in the melt. Figure 6c, in which the Rayleigh number based on ΔT and the decreasing depth of the liquid region is plotted as a function of time, helps to determine the strength of convection within the chamber. When the magma is initially emplaced it is quiescent, and a thermal,
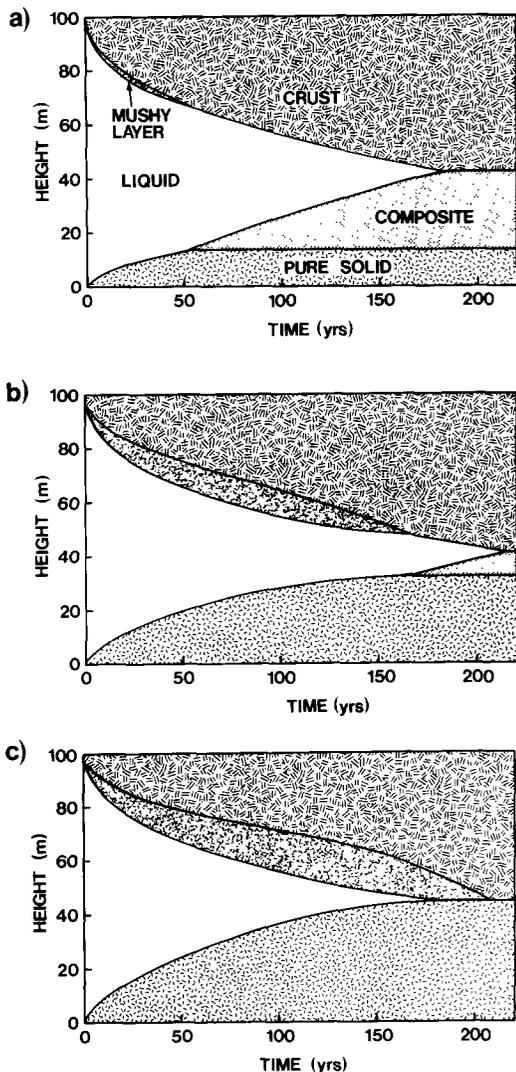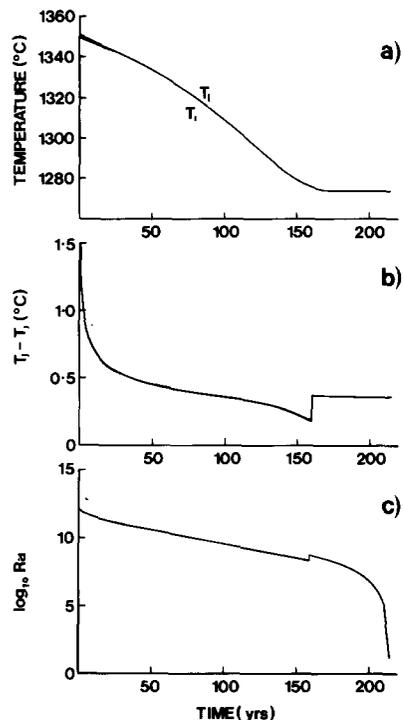
Fig. 6. (a) The temperatures of the melt, T_1, and of the interface between the mushy layer and the melt, T_i, as functions of time for a 100 m thick layer of $Di_{80}An_{20}$ intruded into country rock initially at $0\,^\circ C$. Note the discontinuity in slope at 160 yr, after which time the interior temperature is maintained at the eutectic value of $1274\,^\circ C$. Even though T_i is only slightly less than T_1, the difference ΔT, shown in (b), is sufficient to drive vigorous convective motions within the molten magma. The corresponding values of the Rayleigh number of the melt as a function of time are shown in (c). The discontinuity at 160 years is due to the change in interior dynamics when the eutectic temperature is achieved in the melt.

Fig. 5. The growth of solid as a function of time for magma in a chamber 100 m high intruded at its liquidus into country rock at $0\,^\circ C$. The three diagrams indicate the different evolutions experienced by intrusions of different initial compositions C_0 and hence liquidus temperatures T_L. (a) $C_0 = 65\%Di$, $T_L = 1308\,^\circ C$; (b) $C_0 = 80\%Di$, $T_L = 1352\,^\circ C$; (c) $C_0 = 95\%Di$, $T_L = 1382\,^\circ C$.

conductive boundary layer develops at the cooled roof. The thickness of the boundary layer δ is proportional to $(\kappa t)^{1/2}$ and thus increases with time. Once the local Rayleigh number based on δ exceeds a critical value, as determined by Smith [24] for example, the boundary layer breaks down and the magma begins to convect. For the magma chamber considered here, this occurs after a few hours, which is an insignificant time compared with the overall time of evolution of the chamber. The very large Rayleigh numbers displayed in Fig. 6c signify that the convection will be vigorous after the early transient period just described, until very near the end of the evolution when the
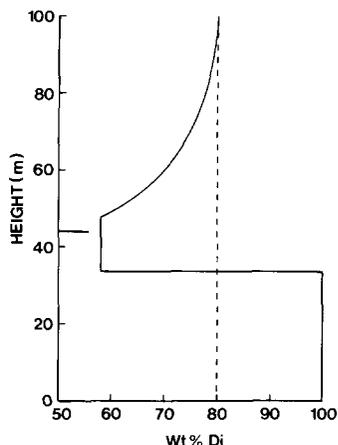
Fig. 7. The bulk composition of a solidified intrusion as a function of depth. The magma had an initial composition of $Di_{80}An_{20}$, as marked on the figure. The horizontal mark at a height of 44 m indicates the level at which the solid grown downwards from the roof meets the solid grown upwards from the floor.

Rayleigh number decreases rapidly due mainly to the shrinking size of the remaining liquid region.

Finally, in Fig. 7, we show a typical variation in final composition of the solidified intrusion. Within the upper layer the proportion of diopside decreases from the initial concentration of the uniform melt to the eutectic composition. The lower layer is mostly pure diopside, by assumption. If the lower layer instead comprised an open crystal pile then its bulk composition would be lower and might vary with height. A more detailed analysis of the formation of the lower layer remains to be carried out. Between these two layers there is a central layer of eutectic composition ($Di_{58}An_{42}$). Our results are quite dependent on the specific phase diagram of the magma. Different results might be expected for a solid solution, for example, than for systems with an almost vertical solidus such as the Di–An system considered here.

5. Discussion

Our results indicate that the extent of internal cooling and differentiation in magma chambers depends on the chamber size as does the relative amount of crystallization at the roof and floor. For small bodies of magma such as lava flows, lava lakes and thin sills, the relative amount of

internal and bottom crystallization is small and the predominant growth of crust occurs at the roof. When cooling occurs at both the floor and roof, as in a sill, a relatively symmetrical growth could be expected with some limited internal differentiation. Settling of phenocrysts which were initially suspended in the magma should however cause some asymmetry and enhancement of the floor layer (as discussed in [25]). For large magma bodies (hundreds to thousands of metres) the internal crystallization becomes substantial. As chamber size increases, crystallization at the floor will become increasingly important and significant internal differentiation can be expected. Geological observations help constrain the dimensions of magma chambers where convection plays a predominant role in internal differentiation. The Tasmanian dolerite [26] and the Palisades sill [27] are intrusions about 300 m thick. Profiles of chemical composition in these intrusions indicate that floor crystallization was predominant over roof crystallization and that substantial internal differentiation took place. In the case of the Palisades sill the floor rocks are approximately seven times thicker than equivalent rocks at the roof and the variation of Mg/(Mg + Fe) within the sill suggests internal cooling of the order of 200°C. Similar conclusions can be deduced from data on the Tasman sill. In the highly differentiated Skaergaard intrusion, the proportion of crystals formed at the floor greatly exceeds those formed at the roof [28], even though the cooling is predominantly from above [29]. Thus our results fit in broadly with observations.

Our results contrast with recent opinions presented by Marsh [25] and Brandeis and Marsh [6]. The essence of their view is that once the interior of the magma chamber is at or below the liquidus, convection ceases or becomes so weak that significant cooling and differentiation cannot occur in the interior. Their argument appears to be that high values of the dynamic viscosity in the thermal boundary layer prevent the formation of plumes. However, a non-dimensional criterion to determine whether this is the correct conclusion is needed. Our investigations demonstrate that the appropriate Rayleigh number is easily large enough to drive vigorous convection and that their view is therefore incorrect. It is true that the convective heat flux from the interior to the roof

quickly becomes small in comparison with the conductive flux through the roof—the flux F plays only a minor role in equation (2) describing the heat budget near the roof. This was discussed at length in [8]. However, the convective heat flux F plays a dominant role in equation (4), which describes the heat balance in the interior of the chamber. It is erroneous to conclude that convection is non-existent simply because the convective heat transfer contributes little to the heat budget at one particular location (the roof). Convection is a dynamic phenomenon, it keeps the magma stirred, it may keep crystals in suspension and it transports other properties than just heat. As was shown in [1], even very small temperature differences yield extremely large Rayleigh numbers given the large dimensions of typical magma chambers. Vigorous convection is therefore nearly always a feature of the dynamics of magma chambers and its effects must be taken into account. For example, we have shown (Fig. 2) that if the convective heat flux were zero (as Marsh would have us believe), then the magma would not cool below its liquidus, there would be no internal crystallization and the magma would not differentiate. We have shown further that convection, coupled with the effects of kinetic undercooling, can cause cooling of the magma below its initial liquidus, internal crystallization and differentiation. These effects have been observed and quantified in the laboratory and are features of many magmatic intrusions. In addition, the erroneous arguments put forward by Marsh [25] and Brandeis and Marsh [6] are not consistent with the observations cited earlier that many intrusions solidify predominantly at the floor despite being cooled mainly through the roof and that they are highly differentiated. This is discussed in greater detail by Sparks [30].

There are several reasons for believing that our model, which incorporates crystallization at the roof in a mushy zone, underestimates the amount of internal cooling, differentiation and floor crystallization. First, in all geological situations there will be additional cooling through the floor. Secondly, the intensity of convection and associated heat fluxes will be substantially larger if crystallization near the roof forms a suspension that can be swept away. With larger convective heat fluxes, crystallization at the roof and growth of the crust
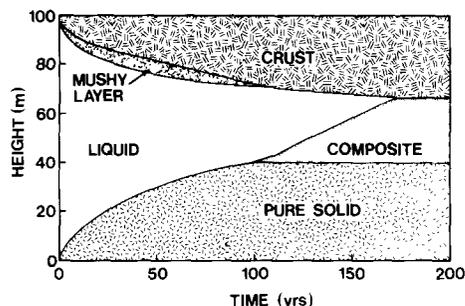

Fig. 8. The growth of solid as a function of time for a magma of composition $Di_{80}An_{20}$ intruded into country rock initially at $0°C$. The growth-rate parameter G was calculated in terms of the viscosity of the melt, given by eqn. (5). This figure should be compared and contrasted with Fig. 3b, for which the results were computed using a growth-rate parameter calculated in terms of the viscosity of a melt of pure diopside, as given by eqn. (2).

will be inhibited and internal cooling, differentiation and bottom crystallization enhanced. For example, Huppert and Sparks [31] demonstrate that the chilled margin can eventually be melted back if the roof region is treated as a suspension zone. The complete absence of a roof sequence is a characteristic of the largest intrusions [28,32–34]. Thirdly, there is the pressure effect on the liquidus which should increase crystallization at the floor relative to that at the roof [32]. Fourthly, the settling out of pre-existing phenocrysts will enhance the proportion at the floor.

We have made computations of a solidifying Di–An melt in which we used a kinetic growth law measured for pure diopside [17]. We note that if $\mu = \rho_l \nu$, with ν given by equation (5), is used in the growth law (1) in place of expression (2) then the results presented in Fig. 8 are obtained for the case of a melt of composition $Di_{80}An_{20}$ solidifying in a chamber 100 m deep. These are significantly different from the results obtained and illustrated in Fig. 3b; in particular, a much greater proportion of the chamber is predicted to have solidified at the floor. Since the viscosity of a Di–An melt increases appreciably as the proportion of An increases between a melt of pure diopside and a melt of eutectic composition, the computed growth rate is much smaller for a given undercooling, which causes the growth at the roof to slow down relative to the growth at the floor. However, it is not known how the growth parameter G varies with composition, so we hesitate to

conclude that the system would evolve at rates closer to those shown in Fig. 8 than to those shown in Fig. 3b. This calculation does, however, indicate the need to measure kinetic growth rates for a wider variety of mineral systems before accurate quantitative predictions can be made.

We conclude that even in the least favourable situation of a mushy zone forming at the roof, convection has a significant role in the internal cooling and differentiation of magma in a magma chamber. Similar dynamics will control the evolution of lava lakes, though the details will be different because the top of the crust of the lake is maintained at a fixed temperature. We plan to present a quantitative investigation of such situations in the future.

Acknowledgements

References

1 H.R. Shaw, Comments on viscosity, crystal setting, and convection in granitic magmas, Am. J. Sci. 263, 120–152, 1965.

2 R.W. Bartlett, Magma convection, temperature distribution, and differentiation, Am. J. Sci. 267, 1067–1082, 1969.

3 C.R. Carrigan, Time and temperature dependent convection models of cooling reservoirs: application to volcanic sills. Geophys. Res. Lett. 11, 693–696, 1984.

4 G. Brandeis and C. Jaupart, On the interaction between convection and crystallization in cooling magma chambers, Earth Planet. Sci. Lett. 77, 345–361, 1986.

5 A.R. McBirney, Mixing and unmixing of magmas, J. Volcanol. Geotherm. Res. 7, 357–371, 1980.

6 G. Brandeis and B.D. Marsh, The convective liquidus in a solidifying magma chamber: a fluid dynamic investigation, Nature 339, 613–616, 1989.

7 B.D. Marsh, On convective style and vigor in sheet-like magma chambers. J. Petrol. 30, 479–530, 1989.

8 J.S. Turner, H.E. Huppert and R.S.J. Sparks, Komatiites II: Experimental and theoretical investigations of post-emplacement cooling and crystallization, J. Petrol. 27, 397–437, 1986.

9 R.C. Kerr, A.W. Woods, M.G. Worster and H.E. Huppert, Disequilibrium and macrosegregation during solidification of a binary melt, Nature 340, 357–362, 1989.

10 R.C. Kerr, A.W. Woods, M.G. Worster and H.E. Huppert, Solidification of an alloy cooled from above. Part I. Equilibrium growth, J. Fluid Mech. 216, 323–342, 1990.

11 R.C. Kerr, A.W. Woods, M.G. Worster and H.E. Huppert, Solidification of an alloy cooled from above. Part II. Nonequilibrium interfacial kinetics, J. Fluid Mech. 217, 331–348, 1990.

12 R.C. Kerr, A.W. Woods, M.G. Worster and H.E. Huppert, Solidification of an alloy cooled from above. Part III. Compositional stratification within the solid, J. Fluid Mech. 218, 337–354, 1990.

13 H.E. Huppert and R.S.J. Sparks, Melting the roof of a magma chamber containing a hot, turbulently convecting fluid, J. Fluid Mech. 188, 107–131, 1988.

14 H.E. Huppert and R.S.J. Sparks, The generation of granitic magmas by intrusion of basalt into continental crust. J. Petrol. 29, 588–624, 1988.

15 H.E. Huppert and R.S.J. Sparks, The fluid dynamics of crustal melting by injection of basaltic sills, Trans. R. Soc. Edinburgh: Earth Sci. 79, 237–243, 1988.

16 D.F. Weill, R. Hon and A. Navrotsky, The igneous system $CaMgSi_2O_6-CaAl_2Si_2O_8-NaAlSi_3O_8$: variations on a classic theme by Bowen, in: Physics of Magmatic Processes, R.B. Hargraves, ed., Princeton University Press, N.J., 1980.

17 R.J. Kirkpatrick, G.R. Robinson and J.F. Hays, Kinetics of crystal growth from silicate melts: anorthite and diopside, J. Geophys. Res. 81, 5715–5720, 1976.

18 R.J. Kirkpatrick, Kinetics of crystal growth in the system $CaMgSi_2O_6-CaAl_2SiO_6$, Am. J. Sci. 274, 215–242, 1974.

19 K.C. Stengel, D.S. Oliver and J.R. Booker, Onset of convection in a variable-viscosity fluid. J. Fluid Mech. 120, 411–431, 1982.

20 F.M. Richter, H.-C. Nataf and S.F. Daly, Heat transfer and horizontally averaged temperature of convection with large viscosity variations. J. Fluid Mech. 129, 173–192, 1983.

21 P.M. Bruce, Thermal convection within the Earth's crust. Ph.D. dissertation, Cambridge, 1989.

22 M.G. Worster, Solidification of an alloy from a cooled boundary, J. Fluid Mech. 167, 481–501, 1986.

23 J.S. Turner, Buoyancy Effects in Fluids, Cambridge University Press, London, 1979.

24 M.K. Smith, Thermal convection during the directional solidification of a pure liquid with variable viscosity, J. Fluid Mech. 547–570, 1988.

25 B.D. Marsh, Crystal capture, sorting and retention in convecting magma, Geol. Soc. Am. Bull. 100, 1720–1737, 1988.

26 J.C. Jaeger and G. Joplin, Rock magnetism and the differentiation of a dolerite sill, J. Geol. Soc. Aust. 2, 1–9, 1955.

27 D.N. Shirley, Differentiation and compaction in the Palisades sill, New Jersey, J. Petrol. 28, 835–866, 1987.

28 L.R. Wager and G.M. Brown, Layered Igneous Rocks, Oliver and Boyd, Edinburgh, London, 1968.

29 D. Norton and H.P. Taylor Jr., Quantitative simulation of the hydrothermal systems of crystallizing magmas on the basis of transport theory and oxygen isotope data: an analysis of the Skaergaard intrusion, J. Petrol. 20, 421–486, 1979.

30 R.S.J. Sparks, Discussion of 'Crystal capture, sorting, and retention and convecting magma' by B.D. Marsh, Geol. Soc. Am. Bull. 102, 847–850, 1990.

31 H.E. Huppert and R.S.J. Sparks, Chilled margins in igneous rocks. Earth Planet. Sci. Lett. 92, 397–405, 1989.

32 T.N. Irvine, Magmatic infiltration metasomatism, double-diffusive fractional crystallization, and adcumulus growth in The Muskox and other layered intrusions, in: Physics of Magmatic Processes, R.B. Hargraves, ed., pp. 325–83, Princeton University Press, Princeton, N.J., 1980.

33 J.R. Wilson and S.B. Larsen, Two-dimensional study of a layered intrusion—the Hyllingen Series, Norway, Geol. Mag. 122, 97–124, 1985.

34 H.H. Hess, Stillwater igneous complex, Montana, a quantitative mineralogical study, Geol. Soc. Am. Mem. 80, 1960.